

# A Mass Flowrate Correlation for Refrigerants and Refrigerant Mixtures Flowing Through Short Tubes

W. Vance Payne<sup>1</sup>, Dennis L. O'Neal<sup>2</sup>

<sup>1</sup>National Institute of Standards and Technology  
Building 226, Room B114, MS 8631  
Gaithersburg, MD USA 20899

<sup>2</sup>Department of Mechanical Engineering  
Texas A&M University  
College Station, Texas USA 77843

## ABSTRACT

This investigation examined mass flowrate of R12, R134a, R502, R22, R407C, and R410A through short tubes. Short tube length ranged from 9.5 mm to 25.4 mm, and sharp edged diameters ranged from 1.09 mm to 1.94 mm. The correlation covers both single-phase and two-phase entrance conditions under approximately choked flow. The correlation consists of non-dimensional parameters that are a function of upstream conditions, downstream conditions, short tube geometry, and critical point pressure/temperature. The correlated data were drawn from previous work and work performed during this investigation. The general form of the correlation is a function for single-phase flow multiplied by a function incorporating parameters for two-phase flow. Over 1200 data points were used to produce the correlation.

## INTRODUCTION

Designers need a generalized correlation for refrigerant mass flow through a short tube orifice. One that would be applicable to a wide range of refrigerants would be very useful and preclude reprogramming as the refrigerant choice changed. Such a correlation would aid in system design and allow the examination of a full range of refrigerant choices. This work attempts to correlate the mass flowrate of several different refrigerants into a single closed-form equation capable of predicting mass flowrate over the range of conditions seen in air-conditioning applications. The data used in this effort were taken from previous work performed at the Energy Systems Laboratory of Texas A&M University combined with data generated during this investigation.

Short tubes are used in vapor compression cycles to meter refrigerant flow. The short tube is a constant area restriction with a sharp edge or a chamfered entrance. Inlet chamfering has a dramatic effect upon mass flowrate (Aaron and Domanski 1990, Kim 1993). Mass flowrate through a short tube can be modeled by the single-phase orifice equation:

$$\dot{m} = KA\sqrt{2g\rho(P_{up} - P_{down})} \quad (1)$$

where  $\dot{m}$  = mass flowrate  
K = orifice constant  
A = orifice area  
g = gravitational force per unit mass  
 $\rho$  = fluid density  
P = upstream and downstream pressure, respectively.

Mass flow characteristics of the short tube have been studied by many investigators (Burnell 1947, Bailey 1951, Kinderman and Wales 1957, Zaloudek 1963, Mei 1982, Krakow 1988). Recent works have focused on the mass flow characteristics of HFC refrigerants (Kim and O'Neal 1993, EPA 1995).

Analytical models of short tube flow can be characterized by the homogeneous equilibrium method (HEM), homogenous frozen method (HFM), and non-homogenous equilibrium method (NEM). Hsu and Graham 1976, Henry 1979, and Deihaye et al. (1981) give good summaries of many works that may be characterized by the above methods.

## **EXPERIMENTAL APPARATUS**

A schematic diagram of the experimental setup is shown in Figure 1. A complete description of the test facility can be found in Kim (1994) and Payne and O’Neal (1998). The test loop was designed to allow control of each operating parameter such as upstream subcooling or quality, upstream pressure, and downstream pressure. Three major flow loops were used: (1) a refrigerant flow loop containing the test section, (2) a hot water flow loop supplying the evaporation heat exchanger and (3) a chilled water-glycol flow loop supplying the condensation heat exchanger.

A diaphragm liquid pump with a variable speed motor was used to circulate the refrigerant. The diaphragm pump did not require lubrication as would a compressor. The pressure entering the test section (upstream or condenser pressure) was controlled by adjusting the speed of the refrigerant pump and by bypassing liquid refrigerant from the pump to the short tube exit.

The refrigerant subcooling or quality entering the test section was set by a water heated heat exchanger (evaporation heat exchanger) and an electric heat tape. For single-phase conditions at the inlet of the test section, most of the energy transfer to the refrigerant was supplied by the evaporation heat exchanger. A heat tape with adjustable output from 0 to 900 W was utilized to provide precise control of upstream subcooling. For two-phase flow conditions at the inlet of the test section, the flow from the pump was heated by the evaporation heat exchanger to 1.1 °C of subcooling, and a heat tape was used to reheat the refrigerant to the desired inlet quality.

Two-phase refrigerant exiting the test section was condensed and subcooled in the water/glycol cooled heat exchanger (condensation heat exchanger) so that the refrigerant pump had only liquid at its suction side. A liquid receiver was used before the refrigerant pump to ensure only liquid entered the pump. The pressure at the exit of the test section (downstream or evaporator pressure) was controlled by adjusting the temperature and flow rate of chilled water/glycol entering the heat exchanger.

A typical sharp edged short tube is shown in Figure 2. The short tubes used in this investigation are listed in Table 1.

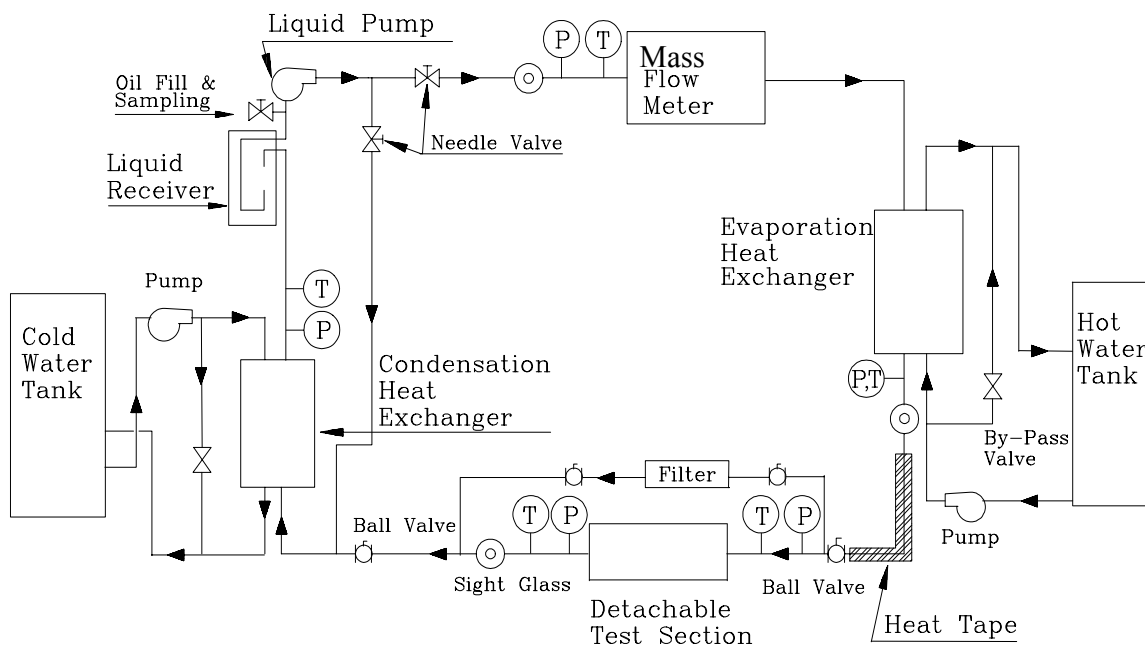


Figure 1: Schematic diagram of the short tube test apparatus

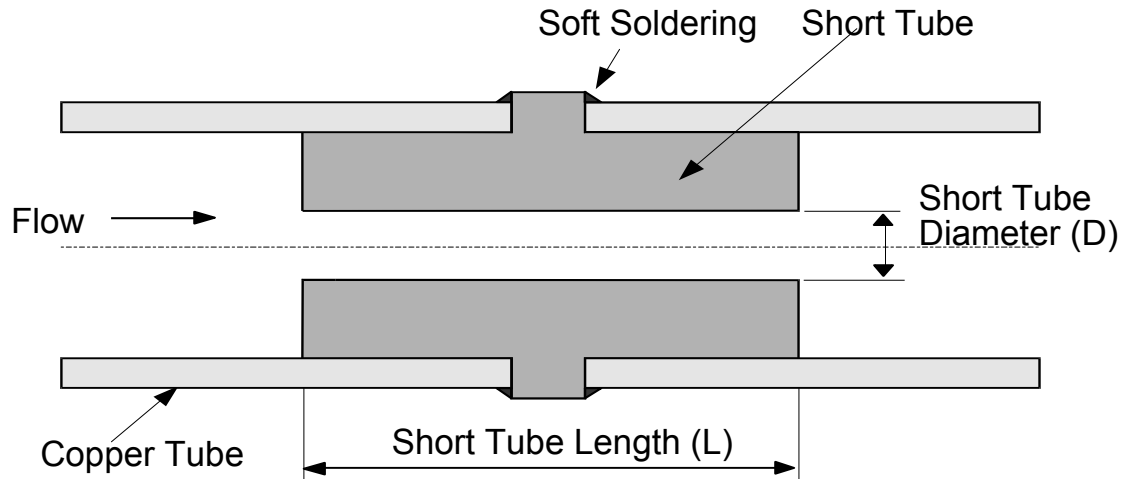


Figure 2: Schematic of a short tube test section

Table 1: Dimensions of the test sections

Length, mm	Diameter, in (mm)
12.7	1.097
12.7	1.341
12.7	1.712
12.7	1.938
19.08	1.095
19.05	1.341
19.08	1.717
19.05	1.935
25.40	1.095
25.40	1.341
25.35	1.717
25.40	1.935

### ***MEASUREMENT UNCERTAINTY***

All of the data used for the correlation were collected under similar conditions. Pressure, temperature, mass flowrate, electric power consumption, length, and diameter were measured. Temperatures were measured by single T-type thermocouples. Pressure was measured adjacent to temperature measurement locations. Mass flowrate was measured by a coriolis effect meter. Pressure fluctuations were considered in the pressure error of the mass flowmeter. Pressure fluctuation for two-phase entrance conditions increased. This was assumed to be caused by density waves, but the fluctuations were still below or equal to 3.4 kPa after pump and by-pass line adjustments. Pressure fluctuations caused mass flowrate to change by less than 2.7 kg/h. The calculation of two-phase quality at the entrance of the test section was performed using an energy balance on the electric heat tape section of the upstream heat exchanger. The correlation predicted mass flowrate for single-phase flow with a median 95 % relative uncertainty of  $\pm 18.8\%$ . Figure 3 shows the goodness of fit of the correlation for several refrigerant and oil mixtures. Oil concentration varied up to a maximum of 3.5 % by mass.

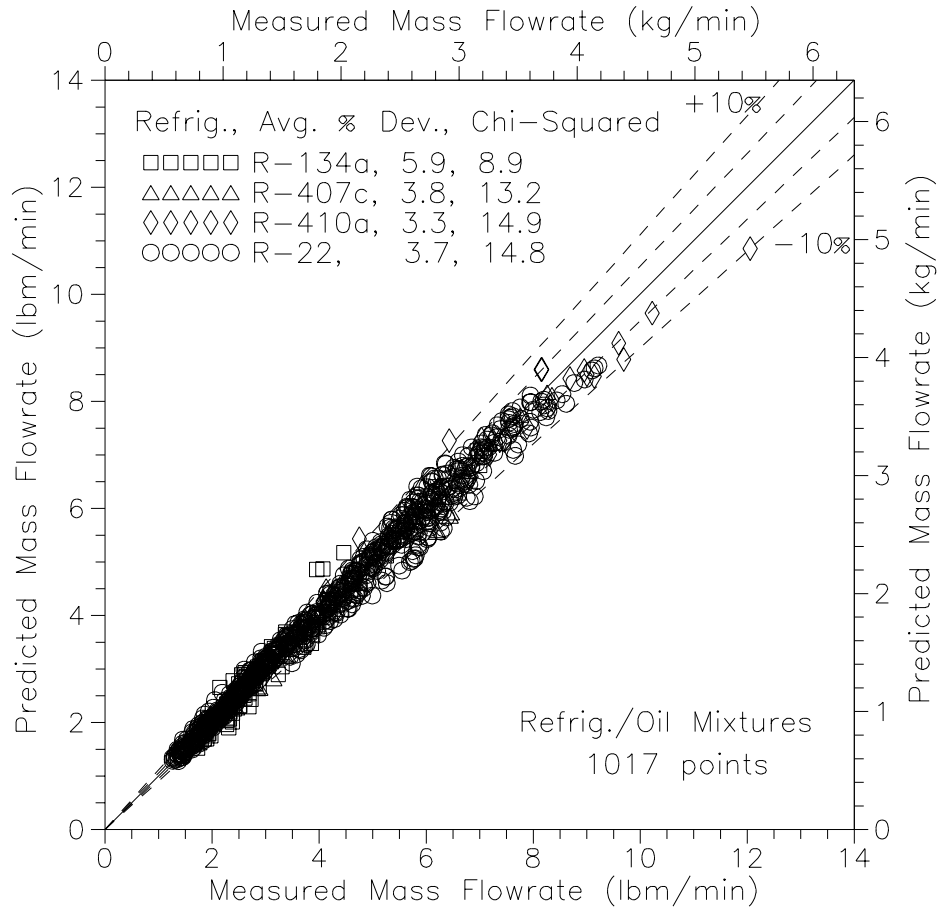


Figure 3: Predicted versus measured mass flowrate for all refrigerant/oil mixture data

### REFRIGERANTS

The refrigerants used to generate the current correlation are described below in Table 2. The extent of the single-phase and two-phase data used to generate the correlation is summarized below in Tables 3 and 4. All of the data summarized below were collected using the experimental apparatus described above. Refrigerant saturation properties were taken from tables supplied by DuPont Fluorochemicals for R407C and R410A (Dupont 1994) or from the ASHRAE Handbook (1993).

Table 2: Characteristics of refrigerants used in the correlation at 1.67 °C

Refrigerant	P <sub>c</sub> , kPa	T <sub>c</sub> , °C	Volumetric Capacity, kJ/m <sup>3</sup>	Chemical Name
R12	4124.9	111.8	2845.0	CCl <sub>2</sub> F <sub>2</sub>
R134a	4055.9	101.0	3018.0	CF <sub>3</sub> CH <sub>2</sub> F
R502	4074.8	82.2	4892.1	R22/115 (CHClF <sub>2</sub> / CClF <sub>2</sub> CF <sub>3</sub> ) 48.8/51.2 by mass
R22	5054.0	96.2	4538.1	CHClF <sub>2</sub>
R407C	4619.1	86.7	4333.2	R32/125/134a (CH <sub>2</sub> F <sub>2</sub> / C <sub>2</sub> HF <sub>5</sub> / CF <sub>3</sub> CH <sub>2</sub> F) 23/25/52 by mass
R410A	4963.0	72.5	7135.1	R32/125 (CH <sub>2</sub> F <sub>2</sub> / C <sub>2</sub> HF <sub>5</sub> ) 50/50 by mass

Table 3: Extent of the pure single-phase data

	Upstream Pressure Range, kPa	Down-stream Pressure Range, kPa	Upstream Temp. Range, °C	Upstream Subcooling Range, °C	Length Range, mm	Diameter Range, mm	Points
R12	841 to 1324	331 to 689	21 to 51	0 to 14	9.5 to 25.4	1.1 to 1.72	43
R134a	883 to 1469	290 to 565	21 to 51	0 to 14	9.5 to 25.4	1.08 to 1.73	272
R502	1482 to 2068	655	21 to 49	0 to 14	12.6 to 25.4	1.1 to 1.72	41
R22	1165 to 2027	469 to 848	21 to 51	0 to 14	9.5 to 25.4	1.08 to 1.94	582
R407C	1517 to 2282	531 to 931	21 to 51	0 to 11	12.7 to 25.4	1.09 to 1.94	173
R410A	2130 to 3185	758 to 1241	21 to 51	0 to 11	12.7 to 25.4	1.09 to 1.94	109

Table 4: Extent of the pure two-phase data

	Upstream Pressure Range, kPa	Down-stream Pressure Range, kPa	Upstream Quality Range, (%)	Length Range, mm	Diameter Range, mm	Points
R134a	883 to 1469	290 to 565	0 – 10.4	9.5 to 25.4	1.08 to 1.73	132
R502	1482 to 2068	655	0 - 9.4	12.6 to 25.4	1.1 to 1.72	26
R22	1165 to 2027	469 to 848	0 – 10.2	9.5 to 25.4	1.08 to 1.94	306
R407C	1517 to 2282	531 to 931	0 - 4.7	12.7 to 25.4	1.09 to 1.94	28
R410A	2130 to 3185	758 to 1241	0 - 8.7	12.7 to 25.4	1.09 to 1.94	25

### EMPIRICAL CORRELATION

The goal of these efforts was to produce an equation to represent the mass flowrate of pure refrigerants flowing through short tubes. The basic equation took the following form:

$$\dot{m} = C_{tp} \dot{m}_{psp} \quad (2)$$

where:  $\dot{m}$  = total mass flowrate, kg / h  
 $C_{tp}$  = ratio of pure two-phase to pure saturated refrigerant flow  
 $\dot{m}_{psp}$  = pure single-phase refrigerant flow.

The above equation was non-dimensionalized with each parameter represented by different functional forms of the important flow parameters. The correlation began with the single-phase flow of pure refrigerants through the short tube. Next, the pure single-phase equation was modified with a multiplier,  $C_{tp}$ , to produce an equation to predict pure two-phase mass flow.

#### Single-Phase Correlation

At the beginning of the modeling process, a large number of refrigerant properties and flow geometry parameters were included to produce non-dimensional groups. To illustrate the process consider a general function. The variables may be arranged in the form of an equation:

$$v_1 = F(v_2, v_3, \dots, v_n) \quad (3)$$

Here  $F()$  is an unspecified function of the  $n-1$  independent variables. The Buckingham Pi theorem states that given a relationship among  $n$  variables as shown in Equation 3, the variables may be grouped into  $n-m$  independent dimensionless ratios defined by Equation 4:

$$\pi_1 = F(\pi_2, \pi_3, \dots, \pi_{n-m}) \quad (4)$$

The number  $m$  is usually, but not always, equal to the number of independent dimensions needed to specify the dimensions of all the variables (Fox and McDonald 1992).

The dimensional analysis began with the selection of parameters which included the main dimensions of length, mass, temperature, and time. For the case of single-phase flow the variables selected which did not form a pi between themselves were  $\rho_f, P_c, T_c,$  and  $D$ .

The resulting non-dimensional groups can be seen in Table 7. Different groupings of the parameters may be realized by choosing different primary variables which do not form a pi among themselves; such as  $\rho_f, \mu_f, D,$  and  $C_{pf}$ .

Table 7: Pure single-phase PI groups

		PI Group	Parameters
1	$\frac{G}{\sqrt{\rho_f P_c}}$	7	$\frac{T_{sub}}{T_c}$
2	$\frac{\mu_f}{\sqrt{\rho_f P_c D^2}}$	8	$\frac{L}{D}$
3	$\frac{\mu_g}{\sqrt{\rho_f P_c D^2}}$	9	$\frac{P_{up}}{P_c}$
4	$\frac{\rho_g}{\rho_f}$	10	$\frac{P_{down}}{P_c}$
5	$\frac{\rho_f h_{fg}}{P_c}$	11	$\frac{P_{sat}}{P_c}$
6	$\frac{\rho_f T_c C_{pf}}{P_c}$		

The parameters  $\rho_f, P_c, T_c,$  and  $D$  were chosen because they provided groups with a small number of variables and included very commonly available critical conditions. Table 7 saturated properties were calculated as a function of the upstream temperature.

The pi groups listed in Table 7 were formed from purely empirical considerations with no respect for the physical significance of the individual parameters. Upon examining the pi groups, it was interesting to note that group 2 and group 3 were the ratio of viscous forces to thermodynamic critical point pressure forces. The density ratio, group 4, can be an indicator of the slip ratio between phases at the short tube exit plane (Wallis 1980). The ratio of energy required for phase change to potential energy at the critical pressure was found in group 5 and group 6. The ratio of upstream subcooling to critical temperature was a completely empirical quantity. The length to diameter ratio was used by several investigators to construct critical flow models (Kim 1993, Aaron and Domanski 1990, Bailey 1951). The remaining three ratios of upstream pressure, downstream pressure, and saturation pressure were completely empirical and do not appear to carry any obvious physical significance.

Many procedures may be used to select the independent variables that should be included in the regression. Some of the basic methods are (1) performing all possible regressions among several functional forms, (2) the backward elimination method using all independent variables, and (3) a forward selection procedure including all of the independent variables (Ott 1984). The first method, where all possible regressions are performed, would require

huge amounts of computing time and would not be an efficient method of determining the proper fit. The backward elimination method would be a reasonable alternative to examining all possible regressions. The backward elimination method was used in a linear combination of the non-dimensional parameters (Equation 5).

$$\pi_1 = b_1 + b_2 * \pi_2 + b_3 * \pi_4 + \dots \quad (5)$$

Those parameters having a T-value with significance greater than 95 % were selected as being important to the correlation. The groups (and their combinations) which survived this elimination procedure are listed below in Table 8.

Table 8: Non-dimensional groups significant to a linear short tube critical mass flowrate correlation

Group	Parameters
$\pi_1$	$\frac{G}{\sqrt{\rho_f P_c}}$
$\pi_2$	$\frac{P_c - P_{up}}{P_c}$
$\pi_3$	$\frac{P_{up} - P_{sat}}{P_c}$
$\pi_4$	$\frac{\mu_f}{\sqrt{\rho_f P_c D^2}}$
$\pi_5$	$\frac{\mu_g}{\sqrt{\rho_f P_c D^2}}$
$\pi_6$	$\frac{\rho_g}{\rho_f}$
$\pi_7$	$\frac{\rho_f h_{fg}}{P_c}$
$\pi_8$	$\frac{\rho_f T_c C_{pf}}{P_c}$
$\pi_9$	$\frac{T_{sub}}{T_c}$
$\pi_{10}$	$\frac{L}{D}$

The next step in the regression procedure was choosing the proper functional form for the correlations. Two categories of functions were considered for the functional forms: (1) power law and (2) rational polynomials. The basic power law equations have been used throughout the engineering literature to represent many different kinds of phenomena. For the pure single-phase correlation, the power law model takes the following form:

$$\pi_1 = a_1 * \pi_2^{a_2} * \pi_3^{a_3} * \dots \quad (6)$$

The power law equation was considered along with another functional form, the rational polynomial.

Rational approximations are mathematically well behaved and can be used to produce accurate correlations to a wide variety of experimental data. The advantages of rational approximations have been advanced by Ray (1991) and Press et al. (1992). Rational approximations improve upon power law equations and simple polynomials by providing better extrapolation characteristics, better interpolation accuracy, and lower order. Rational approximations have been used successfully to represent equations of state for new zeotropic refrigerant mixtures (Perez 1992). These characteristics combined to promote the rational polynomial as a good candidate for correlating multi-phase critical flow data for multiple refrigerants.

A routine was implemented which inserted quadratic, cubic, natural log, natural log squared and natural log cubed of each group into the numerator and then the denominator of the rational polynomial. The routine would begin with the basic equation containing the first ranked group,  $\pi_3$ :

$$\pi_1 = \frac{b_1 + b_2 * \pi_3}{1 + b_3 * \pi_3} \quad (7)$$

First order groups would then be added first to the numerator and then to the denominator until the list of groups was exhausted. If the addition of the extra group to the equation caused a decrease in the error then this equation became the new “best” equation. This continued with every group in Table 8 until the best fit was produced. This method was varied by inserting all the variations of a particular group before moving on to the next group. The best equation produced by these two methods produced the smallest sum of squares of the error.

The criteria for an equation becoming the best equation was set at a 1 % improvement in chi-squared (Equation 8).

$$\chi^2 = \frac{\left( \sum \left( \frac{\text{Calculated} - \text{Measured}}{\text{Error in Measured}} \right)^2 \right)}{N - n - 1} \quad (8)$$

where N = number of experimental measurements  
n = number of adjustable parameters in the correlation.

The first equation processed would be selected as having the “best” chi-squared value. If subsequent equations produced a fit with a lower chi-squared, then the new equation would become the best equation. The full correlation with the largest number of coefficients is listed below. Table 8 defines the pi-groups used for this correlation. The data included approximately 1220 points of pure single-phase mass flow through sharp edged short tube orifices. Refrigerants 12, 134a, 502, 22, 407C and 410A were included in this correlation.

$$\pi_1 = \frac{a_1 + a_2 * \pi_3 + a_3 * \pi_9 + a_4 * \pi_6 + a_5 * \pi_7 + a_6 * \ln(\pi_{10}) + a_7 * [\ln(\pi_{10})]^2 + a_8 * [\ln(\pi_4)]^2}{1 + a_9 * \pi_3 + a_{10} * [\pi_9]^2 + a_{11} * \ln(\pi_{10})} \quad (9)$$

The full correlation of Equation 9 was submitted to a backward elimination technique which removed one coefficient at a time. The resulting model was fit and values of chi-squared and an absolute value percent difference ( $P_{diff}$ ) (Equation 10) were compared to the full correlation.

$$P_{diff} = \left| \frac{\pi_{1,calculated} - \pi_{1,measured}}{\pi_{1,measured}} \right| * 100\% \quad (10)$$

The model which produced a  $P_{diff}$  of less than 5 % with a standard deviation in  $P_{diff}$  comparable to the full correlation was selected as the best reduced pure single-phase correlation. The seven coefficient correlation produced an average  $P_{diff}$  of less than 5 % with a standard deviation comparable to the full correlation. The removal of four coefficients increased chi-squared by 18 %, increased the average  $P_{diff}$  by 8 %, decreased the standard

deviation in  $P_{diff}$  by 2 %, and decreased the maximum  $P_{diff}$  by 18 %. The full correlation and the seven coefficient reduced correlation also differed in the number of independent variables:

$$\text{Full Correlation : } \pi_1 = f(\pi_3, \pi_4, \pi_6, \pi_7, \pi_9, \pi_{10}) \quad (11a)$$

$$\text{Seven Coefficient Correlation : } \pi_1 = f(\pi_3, \pi_6, \pi_9, \pi_{10}) \quad (11b)$$

The seven coefficient reduced correlation removed saturated liquid viscosity and heat of vaporization from the correlation. The seven coefficient reduced correlation is provided below in Equation 12 and Table 11.

$$\pi_1 = \frac{a_1 + a_2 * \pi_3 + a_3 * \pi_9 + a_4 * \pi_6 + a_5 * \ln(\pi_{10})}{1 + a_6 * \pi_3 + a_7 * (\pi_9)^2} \quad (12)$$

Table 11: Seven coefficient reduced pure single-phase correlation

Coeff.	Value	Asymptotic Standard Error	Asymptotic 95 % Confidence Interval	
			Lower	Upper
a <sub>1</sub>	3.8811E-01	6.47034E-03	3.754E-01	4.0080E-01
a <sub>2</sub>	1.1427E+01	8.1456E-01	9.8288E+00	1.3025E+01
a <sub>3</sub>	-1.4194E+01	1.1052E+00	-1.6363E+01	-1.2026E+01
a <sub>4</sub>	1.0703E+00	3.7670E-02	9.9637E-01	1.1442E+00
a <sub>5</sub>	-9.1928E-02	2.5271E-03	-9.6886E-02	-8.6969E-02
a <sub>6</sub>	2.1425E+01	1.7341E+00	1.8022E+01	2.4827E+01
a <sub>7</sub>	-5.8195E+02	4.4452E+01	-6.6917E+02	-4.9474E+02
SSE = 80.93				
$\chi^2 = 10.43$				

The seven coefficient reduced model was a compact function capable of predicting critical mass flowrates. The full correlation and reduced correlation contained second order functions and natural logs. The full correlation and the reduced correlation included quantities that are readily available from saturated property tables of the various refrigerants. Viscosities, enthalpies, and densities used in both models were calculated as a function of the upstream temperature. This correlation was not tested for any data near the critical point.

## Two-Phase Correlation

With the single-phase correlation equation complete, the two-phase multiplier for the single-phase equation was developed. The two-phase multiplier seen in Equation 2 was defined by the following equation:

$$C_{tp} = \frac{\dot{m}_{tp}}{\dot{m}_{sat}} = \frac{\pi_{1 tp}}{\pi_{1 sat}} \quad (13)$$

where  $\dot{m}_{tp}$  = two-phase mass flowrate

$\dot{m}_{sat}$  = mass flowrate with saturated upstream conditions

$\pi_{1 tp}$  = pure two-phase non-dimensional mass flowrate

$\pi_{1 sat}$  = non-dimensional mass flowrate at saturated upstream conditions.

The complete pure single-phase correlation was used to generate the mass flowrate at saturated conditions. The experimentally measured two-phase mass flowrate was then divided by the calculated saturated mass flowrate to produce the experimentally determined value of  $C_{tp}$ .

The parameters listed in Table 12 were non-dimensionalized using the methods described for the pure single-phase correlation. Again  $\rho_f$ ,  $P_c$ ,  $T_c$ , and  $D$  were used to non-dimensionalize the parameters. The resulting of non-dimensional groups and their linear combinations were formed. Subcooled pressure drop, density differences, viscosity differences, etc.. were added to the list of groups in an attempt to produce the best fit.

Average quantities were calculated using the upstream quality, isentropic downstream quality, and isenthalpic downstream quality. The average quantities can be seen below in Equations 14 through 19 (Wallis, 1969).

$$\rho_{mup} = [(1 - x_{up}) / \rho_f + x_{up} / \rho_g]^{-1} \quad (14)$$

$$\rho_{mdown1} = [(1 - x_{down1}) / \rho_{fdown} + x_{down1} / \rho_{gdown}]^{-1} \quad (15)$$

$$\rho_{mdown2} = [(1 - x_{down2}) / \rho_{fdown} + x_{down2} / \rho_{gdown}]^{-1} \quad (16)$$

$$\mu_{mup} = (1 - x_{up}) * \mu_f + x_{up} * \mu_g \quad (17)$$

$$\mu_{mdown1} = (1 - x_{down1}) * \mu_{fdown} + x_{down1} * \mu_{gdown} \quad (18)$$

$$\mu_{mdown2} = (1 - x_{down2}) * \mu_{fdown} + x_{down2} * \mu_{gdown} \quad (19)$$

A description of the parameters used in the above equations and a complete list of parameters used to form the pure two-phase non-dimensional groups may be seen below in Table 12.

Table 12: Pure two-phase quantities used to create non-dimensional groups

Quantity	Description
$x_{up}$	Upstream quality
$x_{down1}$	Downstream quality based upon isenthalpic flow
$x_{down2}$	Downstream quality based upon isentropic flow
$\rho_{mup}$	Mean upstream density, kg/m <sup>3</sup>
$\rho_{mdown1}$	Mean downstream density based upon isentropic flow, kg/m <sup>3</sup>
$\rho_{mdown2}$	Mean downstream density based upon isenthalpic flow, kg/m <sup>3</sup>
$\rho_g$	Saturated vapor density at the upstream pressure, kg/m <sup>3</sup>
$\rho_f$	Saturated liquid density at the upstream pressure, kg/m <sup>3</sup>
$\rho_{gdown}$	Saturated vapor density at the downstream pressure, kg/m <sup>3</sup>
$\rho_{fdown}$	Saturated liquid density at the downstream pressure, kg/m <sup>3</sup>
$\mu_f$	Saturated liquid viscosity at the upstream pressure, kg/(m h)
$\mu_g$	Saturated vapor viscosity at the upstream pressure, kg/(m h)
$\mu_{fdown}$	Saturated liquid viscosity at the downstream pressure, kg/(m h)
$\mu_{gdown}$	Saturated vapor viscosity at the downstream pressure, kg/(m h)
$\mu_{mup}$	Mean upstream viscosity, kg/(m h)
$\mu_{mdown1}$	Mean downstream viscosity based upon isenthalpic flow, kg/(m h)
$\mu_{mdown2}$	Mean downstream viscosity based upon isentropic flow, kg/(m h)
$L$	Length, m
$D$	Diameter, m
$P_{up}$	Upstream pressure, Pa
$P_{down}$	Downstream pressure, Pa
$P_c$	Critical pressure, Pa
$T_c$	Critical temperature, K
$P_{sat}$	Saturation pressure, Pa
$h_{fg}$	Upstream enthalpy of vaporization, kJ/kg
$h_{fgdown}$	Downstream enthalpy of vaporization, kJ/kg

Each of the groups were ranked by the same procedure used with the single-phase correlation. The top twenty non-dimensional groups, which included linear combinations and other important parameters, were kept based upon this ranking procedure. Table 14 lists the non-dimensional groups that remained after the ranking was completed.

The same procedure used to generate the pure single-phase correlation was modified by inserting the new variable names for the pure two-phase non-dimensional groups. The procedure followed the same sequence as performed for the pure single-phase correlation: (1) the highest ranked non-dimensional group was inserted alone into a first order rational polynomial, (2) first order terms of the remaining non-dimensional groups were inserted first in the

Table 14: Non-dimensional groups used in the pure two-phase flow correlation

Group	Parameters	Rank
tp <sub>6</sub>	$\rho_{mup} / \rho_f$	1
tp <sub>34</sub>	$\frac{x_{up}}{1 - x_{up}} \left( \frac{\rho_f}{\rho_g} \right)^{\frac{1}{2}}$	2
tp <sub>1</sub>	$x_{up}$	3
tp <sub>35</sub>	$(P_c - P_{sat}) / P_c$	4
tp <sub>7</sub>	$\rho_g / \rho_f$	5
tp <sub>16</sub>	$\frac{(\mu_{fdown} - \mu_{gdown})}{\sqrt{\rho_f P_c D^2}}$	6
tp <sub>28</sub>	$P_{up} / P_c$	7
tp <sub>5</sub>	$x_{down2} - x_{up}$	8
tp <sub>8</sub>	$\rho_{fdown} / \rho_f$	9
tp <sub>32</sub>	$(P_c - P_{up}) / P_c$	10
tp <sub>4</sub>	$x_{down1} - x_{up}$	11
tp <sub>17</sub>	$\frac{(\rho_{fdown} - \rho_{gdown})}{\rho_f}$	12
tp <sub>36</sub>	$(T_c - T_{up}) / T_c$	13
tp <sub>27</sub>	$L / D$	14
tp <sub>9</sub>	$\rho_{gdown} / \rho_f$	15
tp <sub>29</sub>	$P_{down} / P_c$	16
tp <sub>2</sub>	$x_{down1}$	17
tp <sub>12</sub>	$\frac{\mu_{fdown}}{\sqrt{\rho_f P_c D^2}}$	18
tp <sub>3</sub>	$x_{down2}$	19
tp <sub>20</sub>	$\frac{\mu_{mup}}{\sqrt{\rho_f P_c D^2}}$	20

numerator and then into the denominator with the “best” equation being kept, (3) higher order terms which include squares and cubes of the natural log of each parameter were inserted first into the numerator and then into the denominator, and finally (4) the equation which improved the chi-squared by 1 % or more became the new “best” equation. This procedure produced the complete pure two-phase correlation shown below in Equation 20. The data used to create the pure two-phase correlation includes approximately 517 points of pure two-phase mass flow

through sharp edged short tube orifices. Refrigerants 134a, 502, 22, 407C and 410A were included in this correlation.

$$C_p = \frac{b_1 + b_2 * tp_6 + b_3 * tp_6^2 + b_4 * tp_6^3 + b_5 * (\ln(tp_6))^2 + b_6 * (\ln(tp_{35}))^2 + b_7 * (\ln(tp_{32}))^2 + b_8 * (\ln(tp_{27}))^2}{1 + b_9 * tp_6 + b_{10} * tp_{34} + b_{11} * tp_{28}^3 + b_{12} * tp_{32}^3 + b_{13} * tp_4 + b_{14} * tp_{17}^2} \quad (20)$$

The full correlation of Equation 20 was submitted to a backward elimination technique identical to the one described for the pure single-phase correlation. The resulting model was fit and values of chi-squared and an absolute value percent difference ( $P_{diff}$ ) (Equation 10) for  $C_{tp}$  were compared to the full correlation. The model which produced a  $P_{diff}$  of less than 5 % with a standard deviation in  $P_{diff}$  comparable to the full correlation was selected as the best reduced pure two-phase correlation. A nine coefficient correlation produced an average  $P_{diff}$  of less than 5 % with a standard deviation equal to the complete correlation. The removal of five coefficients increased chi-squared by 17 %, increased the average  $P_{diff}$  by 4 %, and increased the maximum  $P_{diff}$  by 5 %. The full correlation and the nine coefficient reduced correlation also differ in the number of independent variables:

$$\text{Full Correlation : } C_{tp} = f(tp_4, tp_6, tp_{17}, tp_{27}, tp_{28}, tp_{32}, tp_{34}, tp_{35}) \quad (21a)$$

$$\text{Nine Coefficient Correlation : } C_{tp} = f(tp_6, tp_{27}, tp_{28}, tp_{32}, tp_{34}, tp_{35}) \quad (21b)$$

The nine coefficient reduced correlation removed the isenthalpic downstream quality/upstream quality difference and downstream liquid and vapor density difference from the complete correlation. The nine coefficient reduced correlation is provided below in Equation 22 and Table 16.

$$C_p = \frac{b_1 * tp_6 + b_2 * tp_6^2 + b_3 * (\ln(tp_6))^2 + b_4 * (\ln(tp_{35}))^2 + b_5 * (\ln(tp_{32}))^2 + b_6 * (\ln(tp_{27}))^2}{1 + b_7 * tp_6 + b_8 * tp_{34} + b_9 * tp_{28}^3} \quad (22)$$

Table 16: Nine coefficient reduced pure two-phase correlation

Coeff	Value	Asymptotic Standard Error	Asymptotic 95% Confidence Interval	
			Lower	Upper
b <sub>1</sub>	1.1831E+00	5.7703E-02	1.0698E+00	1.2964E+00
b <sub>2</sub>	-1.4680E+00	8.8786E-02	-1.6424E+00	-1.2937E+00
b <sub>3</sub>	-1.5285E-01	2.2630E-02	-1.9729E-01	-1.0841E-01
b <sub>4</sub>	-1.4639E+01	1.7391E+00	-1.8055E+01	-1.1224E+01
b <sub>5</sub>	9.8401E+00	1.2904E+00	7.3060E+00	1.2374E+01
b <sub>6</sub>	-1.9798E-02	2.7238E-03	-2.5147E-02	-1.4449E-02
b <sub>7</sub>	-1.5348E+00	7.3665E-02	-1.6795E+00	-1.3901E+00
b <sub>8</sub>	-2.0533E+00	1.6374E-01	-2.3748E+00	-1.7317E+00
b <sub>9</sub>	-1.7195E+01	1.8755E+00	-2.0878E+01	-1.3512E+01
SSE = 20.8253				
$\chi^2 = 5.2910$				

The nine coefficient reduced model was a compact function capable of predicting the ratio of pure two-phase mass flowrate to pure saturated mass flowrate. The complete correlation and reduced correlation contain third order functions and natural logs. All quantities were evaluated as a function of temperature.

### **SUMMARY**

The equations presented above allow a designer to determine the refrigerant mass flowrate through a sharp edged short tube restrictor given upstream pressure, upstream temperature ( with saturated liquid and vapor properties), downstream pressure (for two-phase inlet conditions), short tube length, and short tube diameter. The correlations are applicable for refrigerants 12, 134a, 502, 22, 407C and 410A.

### **REFERENCES**

- Aaron, D. A. and Domanski, P. A., 1990, Experimentation, analysis, and correlation of refrigerant-22 flow through short tube restrictors, *ASHRAE Trans.*, 96(1): 729-742.
- Ashrae Handbook, 1993, Fundamentals I-P edition, Chapter 17, American Society of Heating, Refrigerating and Air-Conditioning Engineers, Inc., 1791 Tullie Circle, N.E., Atlanta, GA 30329.
- Bailey, J. F., 1951, Metastable flow of saturated water, *Trans. of ASME*, 73: 1109-1116.
- Burnell, J. G., 1947, Flow of boiling water through nozzles, orifices and pipes, *Engineering*, 164: 572-576.
- Deihaye, J., Giot, M., and Reithmuller, M. L., 1981, *Thermohydraulics of two phase systems for industrial design and nuclear engineering*, Washington, DC: Hemisphere Publishing Co., 405-450,
- DuPont, 1994, Personal Communications with Dr. Donald Bivens, (Thermodynamic Properties of AC9000 and AZ20), DuPont Fluoroproducts, Fluorochemicals Lab, Chestnut Run Plaza, Box 80711, Wilmington, DE 19880.
- EPA, 1995, Two-phase flow of two HFC refrigerant mixtures through short tube orifices, Research Triangle Park, NC: National Risk Management Research Laboratory, EPA-600/R-95-168, November.
- Fox, R.W. and McDonald, A.T., 1992, *Introduction to fluid mechanics*, New York, NY: John Wiley & Sons, 4<sup>th</sup> edition, 30-34.

- Henry, R. E., 1979, *Two-phase flow dynamics*, New York, NY: Hemisphere Publishing Co., 102-111.
- Hsu, Y. Y. and Graham, R. W., 1976, *Transport process in boiling and two-phase systems*, New York, NY: Hemisphere Publishing Co., 22-135.
- Kim, Y., 1993a, *Two-phase flow of HCFC-22 and HFC-134a through short tube orifices*, Ph.D. Dissertation, Texas A&M University, College Station, TX 77843.
- Kim, Y. and O'Neal, D.L., 1993b, An experimental study of two-phase flow of HFC-134a through short tube orifices, *Heat Pump and Refrigeration System Design, Analysis, and Applications*, AES Vol 29, ASME Winter Annual Meeting New Orleans, LA.
- Kim, Y. and O'Neal, D.L., 1994a, A semi-empirical model of two-phase flow of refrigerant-134a through short tube orifices, *Experimental Thermal and Fluid Science*, 7(8): 39-46.
- Kim, Y. and O'Neal, D.L., 1994b, The effect of oil on the two-phase critical flow of refrigerant 134a through short tube orifices, *International Journal of Heat and Mass Transfer*, 37(9), 1377-1386.
- Kindermann, W. J. and Wales, E. W., 1957, Fluid flow through two orifices in series III - the parameters of metastable and stable flow of hot water, *Trans. of the ASME*, 79: 183-190.
- Krakow, K.I., and Lin, S. 1988, Refrigerant flow through orifices, *ASHRAE Trans.*, 94(1): 484-506.
- Mei, V. C., 1982, Short tube refrigerant restrictors, *ASHRAE Trans.*, 88(2): 157-68.
- Ott, Lyman, 1984, *An introduction to statistical methods and data analysis*, 2nd Edition, Boston, MA: PWS Publishers, 459-547.
- Payne, W.V. and O'Neal, D.L., 1998, Mass flow characteristics of R-407c through short-tube orifices, *ASHRAE Trans.*, 104(1).
- Press, W. H., Teukolsky, S. A., Vetterling, W. T., and Flannery, B. P., 1992, *Numerical recipes in FORTRAN*, Cambridge: Cambridge University Press.
- Ray, D., 1991, *Analytical and rational approaches to thermophysical property representation of refrigerants*, M. S. Thesis, State University of New York at Stony Brook.
- Wallis, Graham B., 1969, *One-dimensional two-phase flow*, New York, NY: McGraw -Hill Inc., 17-42.
- Wallis, Graham B., 1980, Critical two-phase flow, *International Journal of Multiphase Flow*, 6: 97-112.
- Zaloudek, R. R., 1963, The critical flow of hot water through short tubes, HW-77594, Richland, WA: Hanford Lab.